Journal of Materials Chemistry

Cite this: *J. Mater. Chem.*, 2011, **21**, 16480

www.rsc.org/materials

PAPER

Efficient donor–acceptor type polymer semiconductors with well-balanced energy levels and enhanced open circuit voltage properties for use in organic photovoltaics†

Jang-Yong Lee, Seung-Hee Kim, In-Sung Song and Doo-Kyung Moon*

Received 14th May 2011, Accepted 5th August 2011
DOI: 10.1039/c1jm12145f

Three donor–acceptor type copolymers, poly[9,9′-dioctylfluorene-*alt*-2,5-bis(seleno-2-yl)-2,3-bis(4-hexyloxyphenyl)quinoxaline] (PFSeQ), poly[9-(1′-octylnonylidene)fluorene-*alt*-2,5-bis(seleno-2-yl)-2,3-bis(4-hexyloxyphenyl)quinoxaline] (PAFSeQ), and poly[*N*-9′-heptadecanyl-2,7-carbazole-*alt*-2,5-bis(seleno-2-yl)-2,3-bis(4-hexyloxyphenyl)quinoxaline] (PCSeQ), were synthesized through Suzuki coupling reactions for use as organic photovoltaic materials with high V_{OC} values. In these polymers, selenophene, which has stronger electron-donating property than thiophene, was adopted as a spacer. The polymers had relatively low optical band gaps (<1.9 eV). We investigated bulk heterojunction type polymer solar cells based on the synthesized polymers used as electron donor materials and [6,6]-phenyl C61 butyric acid methyl ester ($PC_{61}BM$) or [6,6]-phenyl C71 butyric acid methyl ester ($PC_{71}BM$) used as the acceptor. The power conversion efficiency (PCE) of the devices was in the range of 1.1–3.3% under AM 1.5G illumination (100 mW cm^{-2}). Among these polymers, PFSeQ exhibited the best device performance with a power conversion efficiency (PCE) of 3.3% upon the introduction of $PC_{71}BM$ as the acceptor. This is the highest performance among photovoltaic materials containing selenophene units.

Introduction

Semiconducting polymers have generated considerable scientific and industrial interest for the past several decades because of their wide range of uses in organic electronics, such as in organic photovoltaics (OPVs),[1–9] organic thin film transistors (OTFTs),[10–12] organic light emitting diodes (OLEDs),[13–17] *etc.* Among these applications, OPVs have especially attracted significant research interest due to the worldwide technical trend towards sustainable development as well as economic feasibility.[18,19] Nevertheless, low power conversion efficiency has been regarded as the most serious obstacle in OPVs.

The PCE value, which is the most important parameter in OPVs, is governed by the short current density (J_{SC}), open circuit voltage (V_{OC}), and fill factor (FF) in an organic solar cell. The typical method for increasing PCE is to improve the photon-harvesting property by decreasing the band gap, which gives rise to increases of the J_{SC} value.[20,21] However, the strategy which excessively focuses on the J_{SC} value has a drawback from the viewpoint of the energy level, since, in general, the HOMO energy level increases and the LUMO energy level decreases as the band gap decreases.[22] Increasing the HOMO energy level induces decrease of the V_{OC}, which lead to decrease of the PCE. Therefore, for high PCE values, the V_{OC} value should be enhanced along with the J_{SC}. Since the V_{OC} is ultimately limited by the difference between the HOMO of the donor and the LUMO of the acceptor, lowering the HOMO energy level of the polymer is the most important factor for reaching a high V_{OC} value.[23,24] Recently, copolymers with low HOMO energy levels have been vigorously investigated since they have oxidative stability as well as high V_{OC} values.[25–28] Especially, since durability is of great concern for an industrial application, stability of materials, in the field of organic electronics, is regarded as an important property of an organic semiconductor.[29,30]

In this study, we synthesized new donor–acceptor type copolymers, *i.e.* PFSeQ, PAFSeQ, and PCSeQ, with high V_{OC} values for use in organic pholtovoltaics. In order to lower the HOMO energy level, fluorene and carbazole derivatives, both of which have low HOMO energy levels, were introduced as electron-donating units. In order to prevent the polymer band gap from increasing, selenophene, which has a stronger electron donating property than thiophene, was adopted as a spacer.[31–35] Quinoxaline was adopted as an electron-withdrawing unit and alkoxybenzene was introduced in quinoxaline as a side chain in order to increase the solubility of the polymers.

Bulk heterojunction-type devices that utilized $PC_{61}BM$ and $PC_{71}BM$ as acceptors were fabricated in order to investigate the photovoltaic properties of PFSeQ, PAFSeQ, and PCSeQ. Devices using the synthesized polymers and PCBM-blend films

Department of Materials Chemistry and Engineering, Konkuk University, 1 Hwayang-dong, Gwangjin-gu, Seoul, 143-701, Korea. E-mail: dkmoon@konkuk.ac.kr; Fax: +82 2 444 0765; Tel: +82 2 450 3498

† Electronic supplementary information (ESI) available. See DOI: 10.1039/c1jm12145f

as active layers displayed a 1.1–3.3% power conversion efficiency. In the devices that used a PFSeQ/$PC_{71}BM$ blend film, in particular, the highest PCE level (3.3%) was detected (V_{OC} = 0.88 V, J_{SC} = 7.9 mA cm^{-2}, FF = 0.48).

Experimental section

Instruments and characterization

All of the reagents and chemicals were purchased from Aldrich and used as received unless otherwise specified. The ^1H NMR (400 MHz) spectra were recorded using a Brüker AMX400 spectrometer in $CDCl_3$, and the chemical shifts were recorded in units of ppm with TMS as the internal standard. The elemental analyses were measured with EA1112 using a CE Instrument. The absorption spectra were recorded using an Agilent 8453 UV-visible spectroscopy system. The solutions that were used for the UV-visible spectroscopy measurements were dissolved in chloroform at a concentration of 10 μg ml^{-1}. The films were drop-coated from the chloroform solution onto a quartz substrate. All of the GPC analyses were carried out using THF as the eluent and a polystyrene standard as the reference. The TGA measurements were performed using a TA Instrument 2050. The cyclic voltammetric waves were produced using a Zahner IM6eX electrochemical workstation with a 0.1 M acetonitrile (substituted with nitrogen for 20 min) solution containing tetrabutylammonium hexafluorophosphate (Bu_4NPF_6) as the electrolyte at a constant scan rate of 50 mV s^{-1}. ITO, a Pt wire, and silver/silver chloride [Ag in 0.1 M KCl] were used as the working, counter, and reference electrodes, respectively. The electrochemical potential was calibrated against Fc/Fc^+. The HOMO levels of the polymers were determined using the oxidation onset value. Onset potentials are values obtained from the intersection of the two tangents drawn at the rising current and the baseline changing current of the CV curves. The LUMO levels were calculated from the differences between the HOMO energy levels and the optical band-gaps, which were determined using the UV-vis absorption onset values in the films.

The current density–voltage (J–V) curves of the photovoltaic devices were measured using a computer-controlled Keithley 2400 source measurement unit (SMU) that was equipped with a Peccell solar simulator under an illumination of AM 1.5G (100 mW cm^{-2}). Thicknesses of the thin films were measured using a KLA Tencor Alpha-step 500 surface profilometer with an accuracy of 1 nm. Topographic images of the active layers were obtained through atomic force microscopy (AFM) in tapping mode under ambient conditions using an XE-150 instrument.

Fabrication and characterization of polymer solar cells

All of the bulk-heterojunction PV cells were prepared using the following device fabrication procedure. The glass/indium tin oxide (ITO) substrates [Sanyo, Japan (10 Ω/γ)] were sequentially lithographically patterned, cleaned with detergent, and ultrasonicated in deionized water, acetone, and isopropyl alcohol. Then the substrates were dried on a hot-plate at 120 °C for 10 min and treated with oxygen plasma for 10 min in order to improve the contact angle just before the film coating process. Poly(3,4-ethylene-dioxythiophene):poly(styrene-sulfonate) (PEDOT:PSS, Baytron P 4083 Bayer AG) was passed through a 0.45 μm filter before being deposited onto ITO at a thickness of *ca.* 32 nm by spin-coating at 4000 rpm in air and then it was dried at 120 °C for 20 min inside a glove box. Composite solutions with polymers and PCBM were prepared using 1,2-dichlorobenzene (DCB). The concentration was controlled adequately in the 0.5 wt% range, and the solutions were then filtered through a 0.45 μm PTFE filter and then spin-coated (500–2000 rpm, 30 s) on top of the PEDOT:PSS layer. The device fabrication was completed by depositing thin layers of BaF_2 (1 nm), Ba (2 nm), and Al (200 nm) at pressures of less than 10^{-6} Torr. The active area of the device was 4.0 mm^2. Finally, the cell was encapsulated using UV-curing glue (Nagase, Japan). In this study, all of the devices were fabricated with the following structure: ITO glass/PEDOT:PSS/polymer:PCBM/BaF_2/Ba/Al/encapsulation glass.

The illumination intensity was calibrated using a standard Si photodiode detector that was equipped with a KG-5filter. The output photocurrent was adjusted to match the photocurrent of the Si reference cell in order to obtain a power density of 100 mW cm^{-2}. After the encapsulation, all of the devices were operated under an ambient atmosphere of 25 °C.

Devices for space-charge-limited current (SCLC) measurements were fabricated in a manner similar to solar cells. The main difference is that in order to facilitate hole-only injection and transport, gold electrodes were deposited instead of the BaF_2/Ba/Al cathode normally used in photovoltaic cells.

Materials

Chloroform was dried over $CaCl_2$, and diethyl ether, THF, and toluene were dried over sodium under a nitrogen atmosphere. The other reagents and chemicals were used as received. 2,Bis(4′,4′,5′,5′-tetramethyl-1′,3′,2′-dioxaborolan-2′-yl)-9,9-dioctylfuorene **1**,[36] 2,7-bis(4′,4′,5′,5′-tetramethyl-1′,3′,2′-dioxaborolan-2′-yl)-9-(1′-decylundecylidene)fluorene **2**,[37] 2,7-bis(4′,4′,5′,5′-tetramethyl-1′,3′,2′-dioxaborolan-2′-yl)-*N*-9′-heptadecanylcarbazole **3**,[38] and 2,3-bis(4-hexyloxyphenyl)-5,8-dibromo-quinoxaline **4** (ref. 39) were prepared as described in the literature.

5,8-Bis(selenophen-2-yl)-2,3-bis(4-hexyloxyphenyl)-quinoxaline 5. To a mixture of **4** (5 g, 7.8 mmol) and 2-(tributylstannyl)-selenophene (7.87 g, 18.7 mmol), $Cl_2(PPh_3)_2Pd$ (5 mol%) and anhydrous THF (30 ml) were added. The reaction flask was evacuated and then filled with nitrogen several times, after which the reaction mixture was refluxed for 24 h. The reaction mixture was cooled to room temperature and poured into water. The mixture was extracted with chloroform and washed with brine. After being dried over anhydrous Na_2SO_4, the solvent was removed by rotary evaporation. The crude product was obtained as a deep red solid after being purified with a silica gel column using hexane/chloroform (3 : 1, v/v) as the eluent. (4.4 g, 76%). ^1H NMR (400 MHz, $CDCl_3$, Me_4Si) δ 0.92 (t, J = 3.6 Hz, 6H), 1.37 (m, 8H), 1.49 (m, 4H), 1.81 (m, 4H), 4.03 (t, J = 8 Hz, 4H), 6.93 (d, J = 9.6 Hz, 4H), 7.27 (d, J = 2.4 Hz, 2H), 7.43 (t, J = 3.6 Hz, 2H), 7.54 (d, J = 8.8 Hz, 4H), 7.59 (d, J = 2.4 Hz, 2H), 8.01 (s, 2H).

5,5′-Dibromo-5,8-bis(selenophen-2-yl)-2,3-bis(4-hexyloxyphenyl)-quinoxaline 6. To a solution of **5** (4.4 g, 5.9 mmol) in DMF (30 ml), NBS (2.32 g, 13 mmol) was added. After the mixture was stirred for 5 h at room temperature, the mixture was poured into

water. The mixture was extracted with chloroform and washed with brine. After being dried over anhydrous Na_2SO_4, the solvent was removed by rotary evaporation. The crude product was obtained as a deep red solid after being purified with a silica gel column using hexane/chloroform (3 : 1, v/v) as eluent. (4.77 g, 90%). ^{1}H NMR (400 MHz, $CDCl_3$, Me_4Si) δ 0.92 (t, $J = 3.6$ Hz, 6H), 1.37 (m, 8H), 1.49 (m, 4H), 1.81 (m, 4H), 4.03 (t, $J = 8$ Hz, 4H), 6.93 (d, $J = 9.6$ Hz, 4H), 7.34 (d, $J = 2.4$ Hz, 2H), 7.54 (d, $J = 8.8$ Hz, 4H), 7.66 (d, $J = 2.0$ Hz, 2H), 8.05 (s, 2H). ^{13}C NMR (400 MHz, $CDCl_3$, Me_4Si) δ 14.09, 22.65, 25.79, 29.29, 31.67, 68.12, 123.14, 123.6, 125.78, 130.12, 131.58, 132.02, 132.11, 136.02, 142.7, 152.45, 160.11.

General procedure of polymerization

To a mixture of $Pd(PPh_3)_4$ (1.0 mol%), monomers (0.7 mmol, respectively), and Aliquat 336 (two or three drops), a degassed mixture of toluene ([monomer] = 0.25 M) and 2 M K_2CO_3 aqueous solution (3 : 2 in volume) was added. The mixture was vigorously stirred at 85–90 °C for 48 h under nitrogen. Bromobenzene and benzylboronic acid were systematically added to the end-cap of the polymer chain. After the mixture was cooled to room temperature, it was washed with a dilute HCl solution, a dilute NH_4OH solution, and water several times. After evaporating the solvent, the crude product was reprecipitated with methanol several times. The polymer was further purified through washing with methanol, acetone, and hexane in a Soxhlet apparatus for 24 h. The chloroform soluble fraction was recovered and dried under a reduced pressure at 50 °C.

PFSeQ. Dark violet solid (0.32 g, 41%). ^{1}H NMR (400 MHz, $CDCl_3$, Me_4Si) δ 0.69 (t, 6H), 0.87 (t, 6H), 1.04 (br, 24H), 1.32 (br, 8H), 1.48 (m, 4H), 1.77 (br, 4H), 1.98 (br, 4H), 3.97 (br, 4H), 6.88 (s, 4H), 7.56–7.68 (br, 12H), 7.98 (br, 2H), 8.15 (br, 2H). Anal. calcd for $C_{69}H_{80}N_2O_2$: C, 73.51; H, 7.15; N, 2.48; O, 2.84. Found: C, 73.17; H, 7.11; N, 2.41; O, 2.97%.

PAFSeQ. Dark violet solid (0.06 g, 8%). ^{1}H NMR (400 MHz, $CDCl_3$, Me_4Si) δ 0.69 (t, 6H), 0.93 (t, 6H), 1.04–2.11 (br, 40H), 2.81 (br, 4H), 4.02 (br, 4H), 6.94 (s, 4H), 7.4–7.9 (br, 12H), 8.04 (br, 2H), 8.22 (br, 2H). Anal. calcd for $C_{70}H_{80}N_2O_2$: C, 73.79; H, 7.08; N, 2.46; O, 2.81. Found: C, 73.21; H, 7.04; N, 2.49; O, 2.92%.

PCSeQ. Dark violet solid (0.45 g, 55%). ^{1}H NMR (400 MHz, $CDCl_3$, Me_4Si) δ 0.66 (t, 6H), 0.84 (t, 6H), 1–1.2 (br, 24H), 1.28 (br, 8H), 1.41 (m, 4H), 1.74 (br, 4H), 1.9 (br, 2H), 2.3 (br, 2H), 3.91 (br, 4H), 4.56(br, 1H), 6.83 (s, 4H), 7.2–8.2 (br, 16H). Anal. calcd for $C_{69}H_{81}N_3O_2$: C, 72.55; H, 7.15; N, 3.68; O, 2.8. Found: C, 72.34; H, 7.11; N, 3.62; O, 2.91%.

Results and discussion

Material synthesis

Scheme 1 shows the synthetic routes of PFSeQ, PAFSeQ, and PCSeQ. The number average molecular weight (M_n) and the weight average molecular weight of PAFSeQ were lower than the others. This was due to the structural rigidity of PAFSeQ. Although planarity was increased by introducing the alkylidene side chain, the sp^2-hybridized carbon at the 9-position of fluorene enhanced the rigidity of the polymer skeleton.[35] This affected the solubility and yield of PAFSeQ. PFSeQ and PCSeQ had good solubilities in common organic solvents, such as chloroform, THF, toluene, chlorobenzene (CB), and *o*-dichlorobenzene (*o*-DCB), while PAFSeQ was partially insoluble parting such solvents. For this reason, the yield of PAFSeQ seriously decreased after Soxhlet extraction.

All of the polymers had decomposition temperatures (T_d) over 330 °C, which indicated that these polymers exhibited good thermal stability, making them applicable for use in polymer solar cells and other optoelectronic devices. The results of the molecular weight measurements and thermal properties are shown in Table 1.

Optical and electrochemical properties

Fig. 1(a) and (b) show the UV-vis absorption spectra of PFSeQ, PAFSeQ, and PCSeQ in a chloroform solution and in thin solid films, respectively. The polymers exhibited maximum UV-vis absorption peaks (λ_{max}) at 543 nm, 543 nm, and 547 nm respectively, in solution. Compared with P3HT's photon absorption property, the three synthesized polymers exhibited lower photon absorption properties than P3HT in the same absorption range as P3HT. However, PFSeQ, PAFSeQ, and PCSeQ exhibited photon absorption in the longer wavelength range of the solar spectrum than did P3HT. Considering that the most photons in the solar spectrum are in the range of 600 nm to 800 nm, the three polymers, PFSeQ, PAFSeQ, and PCSeQ, seemed to have good photon harvesting properties.

As shown in Fig. 1(b), PFSeQ, PAFSeQ, and PCSeQ exhibit similar UV-vis absorption properties in a film. Nevertheless, PFSeQ had the shortest band edge. Comparing PFSeQ with PCSeQ, the band edge of PCSeQ was red-shifted by about 14 nm since polycarbazole had more red-shifted band edge by about 20 nm compared with polyfluorene. Among these polymers, PAFSeQ had the longest UV-vis absorption onset, which stemmed from the increased planarity of its polymer backbone and the electron-donating property from the double bond in the 9-position of fluorene due to introducing the alkylidenefluorene. The optical band gaps of PFSeQ, PAFSeQ, and PCSeQ were calculated from the band edge of the UV-vis absorption spectrum in the film, and they were 1.88 eV, 1.8 eV, and 1.84 eV, respectively.

The electrochemical behavior of the copolymers was investigated with cyclic voltammetry (CV). As shown by the cyclic voltammograms in Fig. 2, the electrochemical oxidation onsets of PFSeQ, PAFSeQ and PCSeQ were 1.4 V, 1.25 V, and 1.35 V, respectively. The reduction parts were not assigned since the reduction peaks were not clear. The HOMO energy levels, which were calculated from the oxidation onsets, were −5.43 eV, −5.28 eV, and −5.38 eV, respectively. The LUMO energy levels were calculated from the difference between the HOMO energy levels and the optical band gap energies. According to the calculations, the LUMO energy levels of PFSeQ, PAFSeQ, and PCSeQ were determined to be −3.55 eV, −3.48 eV, and −3.54 eV, respectively. According to the electrochemical study, the polymers must be air-stable since the HOMO energy levels were below the air oxidation threshold (*ca.* −5.27 eV or 0.57 V *vs.* SCE).[26] Furthermore, this relatively low value assures a relatively high

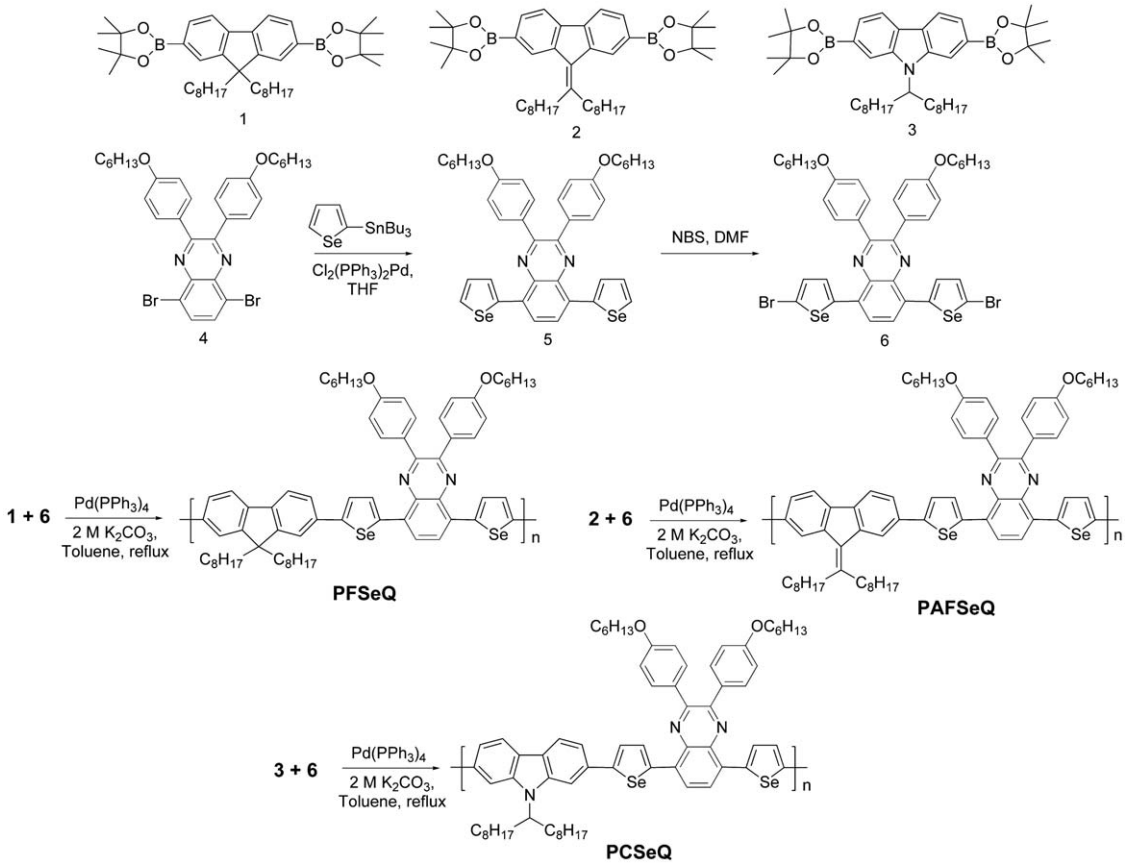

Scheme 1 The synthetic routes of PFSeQ, PAFSeQ, and PCSeQ.

Table 1 Molecular weights[a] and thermal properties

Polymer	Yield (%)	M_n/kg mol^{-1}	M_w/kg mol^{-1}	PDI	T_d/°C
PFSeQ	41	14.9	42.3	2.85	345
PAFSeQ	8	8.3	27.0	3.26	345
PCSeQ	55	13.0	36.1	2.77	336

[a] Molecular weights and polydispersity indexes determined by GPC in THF on the basis of polystyrene calibration.

V_{OC} in the final device. The optical electrochemical properties and calculated energy levels of the synthesized polymers are presented in Table 2.

Morphology analysis

The morphologies of the polymer/PCBM blend films were examined using AFM, as shown in Fig. 3. Dark-colored and light-colored areas correspond to PCBM domains and polymers, respectively. Holes were transferred to anode through p-channels that were composed of polymer materials, and electrons were transferred to cathode through n-channels that were composed of PCBM, therefore, development of detailed p, n-channels was very important. Although all of the blend films showed a smooth surface, large aggregated PCBM domains were obtained in the PAFSeQ/$PC_{61}BM$ film and the film was deficient with respect to detailed p, n-channels compared with the other films, which should be dependent upon the poor solubility of PAFSeQ. In contrast to the PAFSeQ/$PC_{61}BM$ film, PFSeQ and PCSeQ/$PC_{61}BM$ films had detailed p, n-channels.

The polymer/$PC_{71}BM$ blend films formed more detailed p, n-channels than the polymer/$PC_{61}BM$ blend films. In other words, aggregated large $PC_{61}BM$ domains were shown in the polymer/$PC_{61}BM$ blend films, while detailed $PC_{71}BM$ domains were spread in the whole area. The polymer/$PC_{71}BM$ blend films exhibited slightly higher RMS thickness values than the polymer/$PC_{61}BM$ blend films, which could have an effect on the FF of devices.

Hole mobility and photovoltaic characteristics

Hole-only devices (glass/ITO/PEDOT:PSS/polymer:$PC_{71}BM$/Au) were fabricated in order to estimate the hole mobilities of these polymers *via* space-charge-limited current (SCLC) measurements. Hole mobilities of the active layers were calculated from the following SCLC using the *J–V* curves of hole only devices in the dark (Fig. 4).[40] All of photovoltaic cells were fabricated with the bulk heterojunction geometry (BHG) with PCBM. The OPV cells were fabricated with a sandwiched glass/ITO/PEDOT:PSS/polymer-PCBM/BaF_2/Ba/Al structure. A blend of the polymer and $PC_{71}BM$ was dissolved in *o*-DCB, filtered through a 0.45 μm poly(tetrafluoroethylene) (PTFE) filter, and spin coated at 500–1100 rpm for 30 s. The active layers were preannealed at 120 °C for 10 min before electrode deposition. Each substrate was patterned using photolithography techniques in order to produce a segment with an active area of

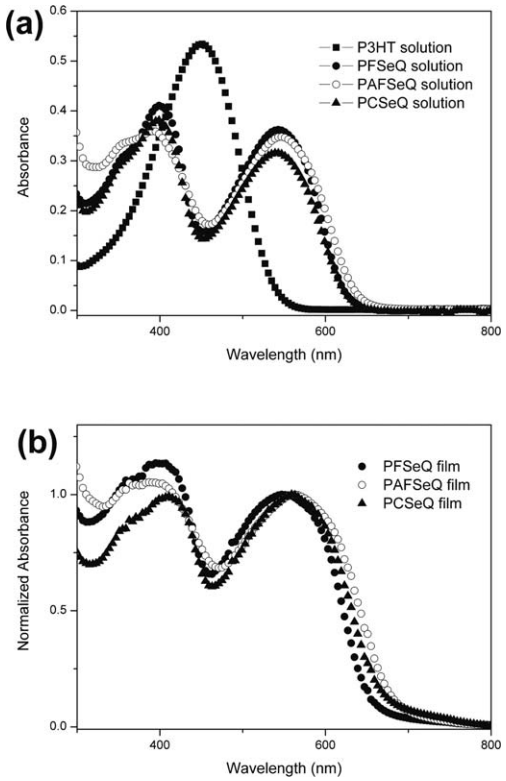

Fig. 1 Comparison of UV-vis absorption spectra of polymers (a) in solution (in chloroform at a concentration of 10 μg ml^{-1}) and (b) in film.

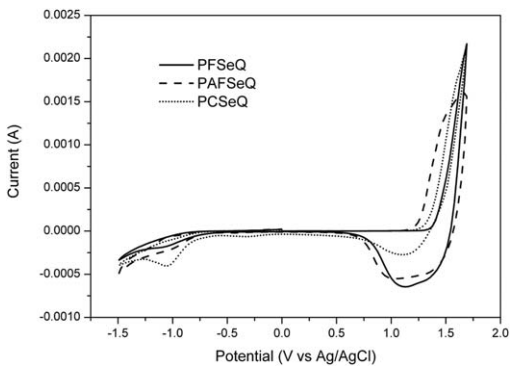

Fig. 2 Cyclic voltammograms of thin films recorded in 0.1 M Bu_4NPF_6/acetonitrile at a scan rate of 50 mV s^{-1}.

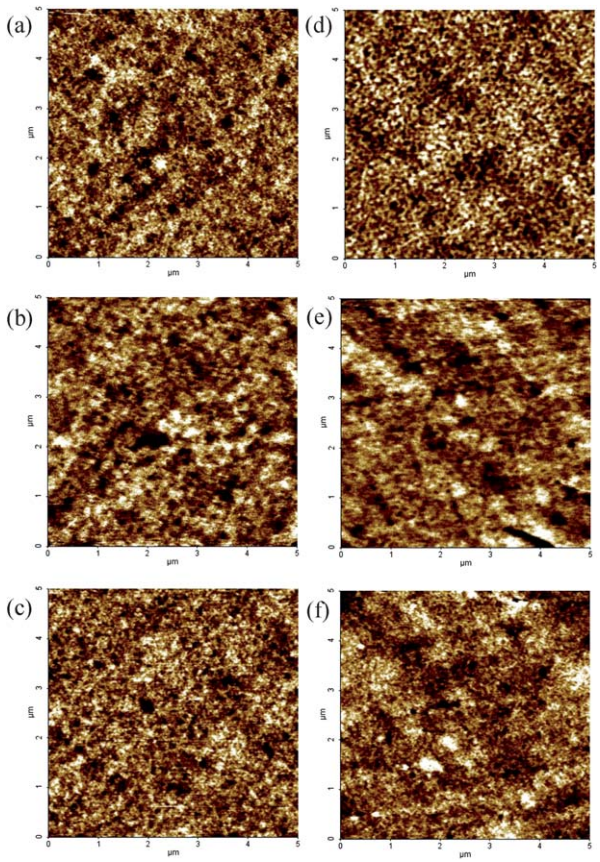

Fig. 3 AFM images of active layer films: (a) PFSeQ/$PC_{61}BM$, (b) PAFSeQ/$PC_{61}BM$, (c) PCSeQ/$PC_{61}BM$, (d) PFSeQ/$PC_{71}BM$, (e) PAFSeQ/$PC_{71}BM$ and (f) PCSeQ/$PC_{71}BM$ blend films.

4.0 mm^2. After all of the fabricated devices were encapsulated in a glove box, the *J–V* characteristics were measured under an ambient atmosphere. Device optimization involved over 40 devices made from over 10 independently prepared polymer/$PC_{71}BM$ films; optimum photovoltaic efficiencies between 3.1% and 3.5% were obtained especially in devices consisted of PFSeQ/$PC_{71}BM$ films.

As shown in Fig. 5, PFSeQ, PAFSeQ, and PCSeQ exhibited V_{OC} values of 0.88 V, 0.78 V, and 0.8 V, and J_{SC} values of 4.8 mA cm^{-2}, 2.7 mA cm^{-2}, and 5.0 mA cm^{-2}, respectively, when $PC_{61}BM$ was used as an acceptor and 80 wt% PCBM was contained in the active layer (1 : 4, w/w). PFSeQ and PCSeQ

Table 2 Optical, electrochemical data, and energy levels of polymers

	UV-vis absorption spectrum					Energy level/eV	
	In $CHCl_3$	In film[a]					
Polymer	λ_{max}/nm	λ_{max}/nm	λ_{onset}/nm	$E_g$op[b]/eV	E_{onset}^{ox}/V	HOMO[c]	LUMO[d]
PFSeQ	543	549	661	1.88	1.40	−5.43	−3.55
PAFSeQ	543	563	688	1.80	1.25	−5.28	−3.48
PCSeQ	547	559	675	1.84	1.35	−5.38	−3.54

[a] Spin-coated from a chloroform. [b] Estimated from the onset of UV-vis absorption data of the thin film. [c] Calculated from the oxidation onset potentials under the assumption that the absolute energy level of Fc/Fc^+ was −4.8 eV below a vacuum. [d] HOMO − E_g^{op}.

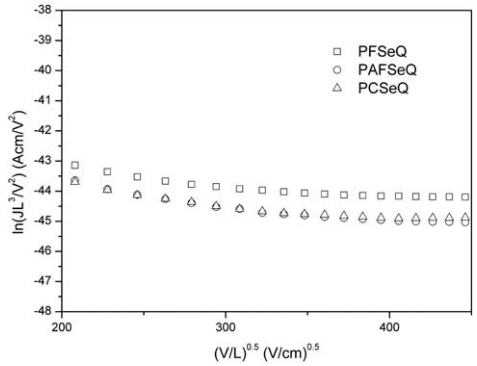

Fig. 4 *J–V* characteristics of the hole-only devices measured in the dark.

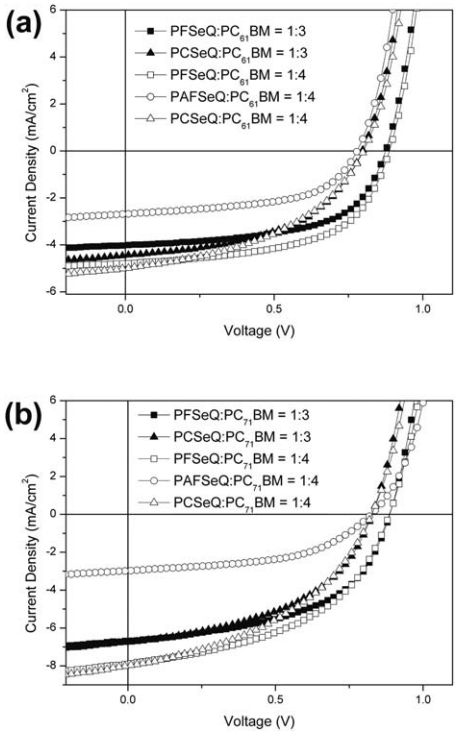

Fig. 5 *J–V* characteristics of photovoltaic devices that have (a) polymer/$PC_{61}BM$ and (b) polymer/$PC_{71}BM$ blend films as active layers.

exhibited similar J_{SC} values. However, PFSeQ had a higher V_{OC} value than did PCSeQ near 0.1 V. This originated from the HOMO energy levels.

The best performance was observed in the device where $PC_{71}BM$ was used as an acceptor and 80 wt% PCBM was contained in the active layer (1 : 4, w/w). In this device, the V_{OC}, J_{SC}, and FF values of PFSeQ were 0.88 V, 7.9 mA cm^{-2}, and 0.48, respectively, thus, the PCE value increased by 3.3%. In the case of the device with PCSeQ, the best performances of 0.84 V for V_{OC}, 7.9 mA cm^{-2} for J_{SC}, 0.48 for FF, and 2.9% for PCE were exhibited under the same conditions as those used for PFSeQ. However, PAFSeQ exhibited a relatively low PCE value of 1.2%. In spite of the improved PCE value upon introducing $PC_{71}BM$ as an acceptor, the FF values were lower than in the polymer/$PC_{61}BM$ device. Considering that the FF value depends on the morphology, as shown in the AFM images, the polymer/

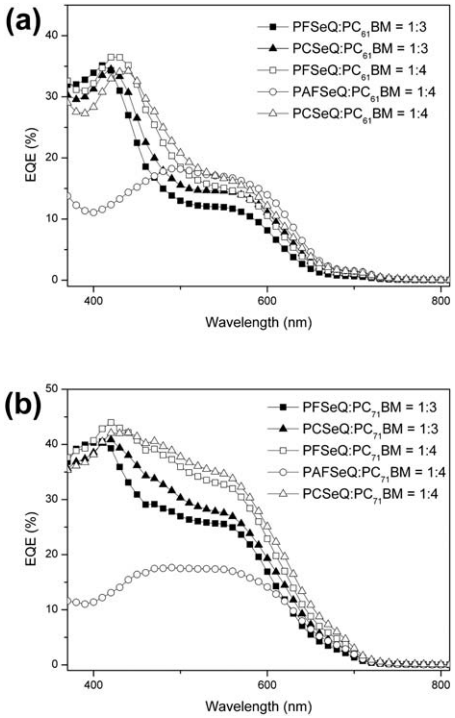

Fig. 6 EQE spectra of photovoltaic devices that have (a) polymer/$PC_{61}BM$ and (b) polymer/$PC_{71}BM$ blend films as active layers.

$PC_{61}BM$ film surfaces were smoother than those of the polymer/$PC_{71}BM$ films, which influences the FF value. However, more detailed p, n-channels were obtained upon introduction of $PC_{71}BM$ to the films, and this likely affected the improved J_{SC} values.

As mentioned above, compared with other polymers, PAFSeQ exhibited a low PCE value of 1.2%, which was chiefly influenced by the J_{SC} value. According to SCLC measurements, PFSeQ (2.45×10^{-6} cm^2 V^{-1} s^{-1}), PAFSeQ (1.47×10^{-6} cm^2 V^{-1} s^{-1}), and PCSeQ (1.21×10^{-6} cm^2 V^{-1} s^{-1}) exhibited analogous values of hole mobilities. This indicated that differences in J_{SC} values were not seriously affected by hole mobilities. Whereas, as shown in Fig. 6, the EQE spectrum of PAFSeQ was greatly different compared with the other two polymers. This means that the low J_{SC} value of PAFSeQ originated from its low EQE value.

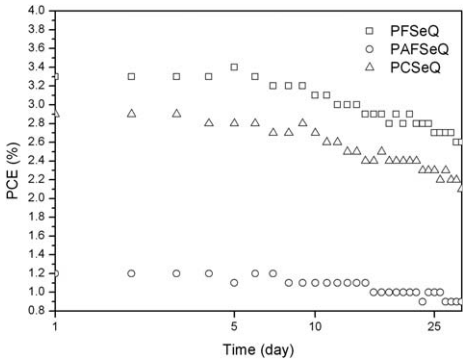

Fig. 7 Durability test data of photovoltaic devices based on PFSeQ, PAFSeQ, and PCSeQ as donor materials.

Table 3 Summary of hole mobilities and photovoltaic characteristics of devices

Active layer (w/w)							
Polymer (P)	Acceptor (A)	Weight ratio (P : A, w/w)	Hole mobility/cm^2 V^{-1} s^{-1}	V_{OC}/V	J_{SC}/mA cm^{-2}	FF	PCE (%)
PFSeQ	$PC_{61}BM$	1 : 3	2.45×10^{-6}	0.88 (±0.02)	4.0 (±0.2)	0.57 (±0.01)	2.0 (±0.2)
		1 : 4		0.88 (±0.02)	4.8 (±0.2)	0.57 (±0.01)	2.4 (±0.2)
	$PC_{71}BM$	1 : 3		0.88 (±0.01)	6.7 (±0.1)	0.52 (±0.01)	3.1 (±0.1)
		1 : 4		0.88 (±0.01)	7.9 (±0.2)	0.48 (±0.01)	3.3 (±0.2)
PAFSeQ	$PC_{61}BM$	1 : 4	1.47×10^{-6}	0.78 (±0.01)	2.7 (±0.2)	0.55 (±0.01)	1.1 (±0.2)
	$PC_{71}BM$	1 : 4		0.82 (±0.01)	3.0 (±0.1)	0.51 (±0.01)	1.2 (±0.1)
PCSeQ	$PC_{61}BM$	1 : 3	1.21×10^{-6}	0.80 (±0.02)	4.5 (±0.2)	0.51 (±0.01)	1.8 (±0.2)
		1 : 4		0.80 (±0.01)	5.0 (±0.3)	0.45 (±0.01)	1.8 (±0.3)
	$PC_{71}BM$	1 : 3		0.82 (±0.02)	6.7 (±0.2)	0.48 (±0.01)	2.7 (±0.1)
		1 : 4		0.84 (±0.01)	7.9 (±0.1)	0.43 (±0.01)	2.9 (±0.1)

In other words, a low PCE value of PAFSeQ depends upon the low J_{SC} value, and the origin of the low J_{SC} value was the low EQE value of PAFSeQ. It was one reason of the low PCE value of PAFSeQ. Another reason was a rigid backbone structure and a low molecular weight of PAFSeQ. A double bond in the 9-position of fluorene reduced the flexibility of the alkyl chains, which resulted in a decrease of solubility. The low solubility exerted a strong influence on the molecular weight. A rigid backbone structure and the low molecular weight restricted intermolecular interaction in solid films, which was likely to be a key factor that limited the PCE value of PAFSeQ.

Photovoltaic devices with $PC_{71}BM$ as an acceptor showed higher EQE values than those with $PC_{61}BM$ as an acceptor, although they absorbed photons in the same range of the solar spectrum. It is because $PC_{71}BM$ has a stronger UV-vis absorption property than does $PC_{61}BM$ in the visible region, especially around 500 nm.[41] As shown in Fig. 6(b), devices where $PC_{71}BM$ was introduced as an acceptor had especially increased EQE around the 500 nm wavelength region. Consequently, the enhanced EQE values due to the introduction of $PC_{71}BM$ resulted in increased absorption in the visible region and detailed p, n-channels greatly affected the J_{SC} value, which influenced the PCE values of devices.

In order to investigate oxidative stability of photovoltaic devices based on three polymers, the current density–voltage (J–V) curves of the devices were measured in ambient conditions for a month. All of the devices were encapsulated to prevent oxidation of the metal electrode and were placed in ambient conditions. As shown in Fig. 7, the PCE values of the devices based on PFSeQ, PCSeQ, and PAFSeQ, respectively, as a donor material had changed little after a week. Moreover, the PCE values of these devices were decreased only about 20% even after a month, which was supposed to originate from electrochemical stability of donor polymers as mentioned above.

The photovoltaic properties of the tested devices are presented in Table 3.

Conclusions

In this paper, three new copolymers—PFSeQ, PAFSeQ, and PCSeQ—with high V_{OC} values were successfully synthesized. In order to improve the photon harvesting properties of these materials by reducing their band gaps, selenophene was introduced in their polymer backbones. The polymers had low band gaps (~1.8 eV) and well balanced energy levels. The best device was the device with a 70 nm thick active layer of PFSeQ mixed with $PC_{71}BM$ in a 1 : 4 ratio, which yielded a V_{OC} value of 0.88 V, a J_{SC} value of 7.9 mA cm^{-2}, a FF value of 0.48, and a high PCE value of 3.3% under simulated sunlight (100 mW cm^{-2}, AM 1.5G). These results relate to well-balanced energy levels, meaning low HOMO and LUMO levels, and good morphological properties. Compared with the other two polymers, PAFSeQ exhibited a relatively low PCE value of 1.2%, which depended on the J_{SC} value that related its morphology and EQE value.

Acknowledgements

This research was supported by a grant from the Fundamental R&D Program for Core Technology of Materials funded by the Ministry of Knowledge Economy, Republic of Korea, and the National Research Foundation of Korea Grant funded by the Korean Government (MEST) (NRF-2009-C1AAA001-2009-0093526).

References

1 T. Y. Chu, J. Lu, Y. Zhang, J. R. Pouliot, S. Wakim, J. Zhou, M. Leclerk, Z. Li, J. Ding and Y. Tao, *J. Am. Chem. Soc.*, 2011, **133**, 4250–4253.
2 K. H. Ong, S. L. Lim, H. S. Tan, H. K. Wong, J. Li, Z. Ma, L. C. H. Moh, S. H. Lim, J. C. de Mello and Z. K. Chen, *Adv. Mater.*, 2011, **23**, 1409–1413.
3 L. Huo, J. Hou, S. Zhang, H. Y. Chen and Y. Yang, *Angew. Chem., Int. Ed.*, 2010, **49**, 1500–1503.
4 C. Piliego, T. W. Holcombe, J. D. Douglas, C. H. Woo, P. M. Beaujuge and J. M. J. Fréchet, *J. Am. Chem. Soc.*, 2010, **132**, 7595–7597.
5 Y. Zhang, S. K. Hau, H. L. Yip, Y. Sun, O. Acton and A. K. Y. Jen, *Chem. Mater.*, 2010, **22**, 2696–2698.
6 R. Mondal, H. A. Becerril, E. Verploegen, D. Kim, J. E. Norton, S. Ko, N. Miyaki, S. Lee, M. F. Toney, J. Brédas, M. D. McGehee and Z. Bao, *J. Mater. Chem.*, 2010, **20**, 5823–5834.
7 H. Y. Chen, J. Hou, S. Zhang, Y. Liang, G. Yang, Y. Yang, L. Yu, Y. Wu and G. Li, *Nat. Photonics*, 2009, **3**, 649–653.
8 H. Xin, X. Guo, F. S. Kim, G. Ren, M. D. Watson and S. A. Jenekhe, *J. Mater. Chem.*, 2009, **19**, 5303–5310.
9 E. Bundgaard and F. C. Krebs, *Macromolecules*, 2006, **39**, 2823–2831.
10 D. H. Kim, B. L. Lee, H. Moon, H. M. Kang, E. J. Jeong, J. I. Park, K. M. Han, S. Lee, B. W. Yoo, B. W. Koo, J. Y. Kim, W. H. Lee, K. Cho, H. A. Becerril and Z. Bao, *J. Am. Chem. Soc.*, 2009, **131**, 6124–6132.
11 S. Allard, M. Forster, B. Souharce, H. Thiem and U. Scherf, *Angew. Chem., Int. Ed.*, 2008, **47**, 4070–4098.

12 B. S. Ong, Y. Wu, Y. Li, P. Liu and H. Pan, *Chem.–Eur. J.*, 2008, **14**, 4766–4778.
13 J. Y. Lee, M. H. Choi, D. K. Moon and J. R. Haw, *J. Ind. Eng. Chem.*, 2010, **16**, 395–400.
14 K. W. Song, J. Y. Lee, S. W. Heo and D. K. Moon, *J. Nanosci. Nanotechnol.*, 2010, **10**, 99–105.
15 K. S. Yook and J. Y. Lee, *J. Ind. Eng. Chem.*, 2010, **16**, 230–232.
16 S. O. Kim, H. C. Jung, M. J. Lee, C. Jun, Y. H. Kim and S. K. Kwon, *J. Polym. Sci., Part A: Polym. Chem.*, 2009, **47**, 5908–5916.
17 J. Liu, Y. Cheng, Z. Xie, Y. Geng, L. Wang, X. Jing and F. Wang, *Adv. Mater.*, 2008, **20**, 1357–1362.
18 F. C. Krebs, T. Tromholt and M. Jørgensen, *Nanoscale*, 2010, **2**, 873–886.
19 F. C. Krebs, J. Fyenbo and M. Jørgensen, *J. Mater. Chem.*, 2010, **20**, 8994–9001.
20 C. Soci, I. W. Hwang, D. Moses, Z. Zhu, D. Waller, R. Gaudiana, C. J. Brabec and A. J. Heeger, *Adv. Funct. Mater.*, 2007, **17**, 632–636.
21 E. Bundgaard and F. C. Krebs, *Sol. Energy Mater. Sol. Cells*, 2007, **91**, 954–985.
22 C. R. Newman, C. D. Frisbie, D. A. da Silva Filho, J. L. Brédas, P. C. Ewbank and K. R. Mann, *Chem. Mater.*, 2004, **16**, 4436–4451.
23 R. Kroon, M. Lenes, J. C. Hummelen, P. W. M. Blom and B. de Boer, *Polym. Rev.*, 2008, **48**, 531–582.
24 A. Gadisa, W. Mammo, L. M. Andersson, S. Admassie, F. Zhang, M. R. Andersson and O. Inganäs, *Adv. Funct. Mater.*, 2007, **17**, 3836–3842.
25 S. H. Park, A. Roy, S. Beaupré, S. Cho, N. Coates, J. S. Moon, D. Moses, M. Leclerc, K. Lee and A. J. Heeger, *Nat. Photonics*, 2009, **3**, 297–302.
26 N. Blouin, A. Michaud, D. Gendron, S. Wakim, E. Blair, R. Neagu-Plesu, M. Belletête, G. Durocher, Y. Tao and M. Leclerc, *J. Am. Chem. Soc.*, 2008, **130**, 732–742.
27 R. Qin, W. Li, C. Li, C. Du, C. Veit, H. Schleiermacher, M. Andersson, Z. Bo, Z. Liu, O. Inganäs, U. Wuerfel and F. Zhang, *J. Am. Chem. Soc.*, 2009, **131**, 14612–14613.
28 E. Wang, L. Wang, L. Lan, C. Luo, W. Zhuang, J. Peng and Y. Cao, *Appl. Phys. Lett.*, 2008, **92**, 033307.
29 M. Manceau, E. Bundgaard, J. E. Carlé, O. Hagemann, M. Helgesen, R. Søndergaard, M. Jørgensen and F. C. Krebs, *J. Mater. Chem.*, 2011, **21**, 4132–4141.
30 M. Jørgensen, K. Norrman and F. C. Krebs, *Sol. Energy Mater. Sol. Cells*, 2008, **92**, 686–714.
31 K. Takimiya, Y. Kunugi, Y. Konda, H. Ebata, Y. Toyoshima and T. Otsubo, *J. Am. Chem. Soc.*, 2006, **128**, 3044–3050.
32 K. Takimiya, Y. Kunugi, Y. Konda, N. Nihara and T. Otsubo, *J. Am. Chem. Soc.*, 2004, **126**, 5084–5085.
33 Y. Kunugi, K. Takimiya, K. Yamane, K. Yamashita, Y. Aso and T. Otsubo, *Chem. Mater.*, 2003, **15**, 6–7.
34 S. Inoue, H. Nakanishi, K. Takimiya, Y. Aso and T. Otsubo, *Synth. Met.*, 1997, **84**, 341–342.
35 Y. M. Kim, E. Lim, I. N. Kang, B. J. Jung, J. Lee, B. W. Koo, L. M. Do and H. K. Shim, *Macromolecules*, 2006, **39**, 4081–4085.
36 R. Yang, R. Tian, J. Yan, Y. Zhang, J. Yang, Q. Hou, W. Yang, C. Zhang and Y. Cao, *Macromolecules*, 2005, **38**, 244–253.
37 M. Heeney, C. Bailey, M. Giles, M. Shkunov, D. Sparrowe, S. Tierney, W. Zhang and I. McCulloch, *Macromolecules*, 2004, **37**, 5250–5256.
38 N. Blouin, A. Michaud and M. Leclerc, *Adv. Mater.*, 2007, **19**, 2295–2300.
39 J. Y. Lee, S. W. Shin, J. R. Haw and D. K. Moon, *J. Mater. Chem.*, 2009, **19**, 4938–4945.
40 S. Jeong, Y. Kwon, B. D. Choi, H. Ade and Y. S. Han, *Appl. Phys. Lett.*, 2010, **96**, 183305.
41 J. Peet, J. Y. Kim, N. E. Coates, W. L. Ma, D. Moses, A. J. Heeger and G. C. Bazan, *Nat. Mater.*, 2007, **7**, 497–500.